Tree Physiology 40, 1355–1365
doi:10.1093/treephys/tpaa080

Research paper

Seasonal fluctuation of nonstructural carbohydrates reveals the metabolic availability of stemwood reserves in temperate trees with contrasting wood anatomy

Morgan E. Furze[1,2,8], Brett A. Huggett[3], Catherine J. Chamberlain[1], Molly M. Wieringa[1], Donald M. Aubrecht[1], Mariah S. Carbone[4,5], Jennifer C. Walker[6], Xiaomei Xu[6], Claudia I. Czimczik[6] and Andrew D. Richardson[5,7]

[1]Department of Organismic and Evolutionary Biology, Harvard University, 26 Oxford St, Cambridge, MA 02138, USA; [2]School of the Environment, Yale University, 195 Prospect St, New Haven, CT 06511, USA; [3]Department of Biology, Bates College, 44 Campus Ave, Lewiston, ME, 04240, USA; [4]Department of Biological Sciences, Northern Arizona University, PO Box 5640, Flagstaff, AZ, 86011, USA; [5]Center for Ecosystem Science and Society, Northern Arizona University, PO Box 5620, Flagstaff, AZ, 86011, USA; [6]Department of Earth System Science, University of California, Irvine, 3200 Croul Hall, Irvine, CA, 92697, USA; [7]School of Informatics, Computing, and Cyber Systems, Northern Arizona University, PO Box 5693, Flagstaff, AZ, 86011, USA; [8]Corresponding author (morgan.furze@yale.edu)

Received March 18, 2020; accepted June 16, 2020; handling Editor Lucas Cernusak

Nonstructural carbohydrates (NSCs) play a critical role in plant physiology and metabolism, yet we know little about their distribution within individual organs such as the stem. This leaves many open questions about whether reserves deep in the stem are metabolically active and available to support functional processes. To gain insight into the availability of reserves, we measured radial patterns of NSCs over the course of a year in the stemwood of temperate trees with contrasting wood anatomy (ring porous vs diffuse porous). In a subset of trees, we estimated the mean age of soluble sugars within and between different organs using the radiocarbon (^{14}C) bomb spike approach. First, we found that NSC concentrations were the highest and most seasonally dynamic in the outermost stemwood segments for both ring-porous and diffuse-porous trees. However, while the seasonal fluctuation of NSCs was dampened in deeper stemwood segments for ring-porous trees, it remained high for diffuse-porous trees. These NSC dynamics align with differences in the proportion of functional sapwood and the arrangement of vessels between ring-porous and diffuse-porous trees. Second, radial patterns of ^{14}C in the stemwood showed that sugars became older when moving toward the pith. The same pattern was found in the coarse roots. Finally, when taken together, our results highlight how the radial distribution and age of NSCs relate to wood anatomy and suggest that while deeper, and likely older, reserves in the stemwood fluctuated across the seasons, the deepest reserves at the center of the stem were not used to support tree metabolism under usual environmental conditions.

Keywords: forest trees, nonstructural carbohydrates, radiocarbon, storage, wood anatomy.

Introduction

Nonstructural carbohydrates (NSC) are used by forest trees for growth and metabolism, but they can also be stored (Dietze et al. 2014, Hartmann and Trumbore 2016). When NSCs (primarily insoluble starch and soluble sugars; soluble sugars herein referred to as sugars) are stored, this reserve enables long-lived, stationary trees to survive during unfavorable environmental conditions when NSC production is impaired. While NSCs have been touted to provide stress tolerance (Myers and Kitajima 2007, Sala et al. 2012, Carbone et al. 2013), we lack a detailed understanding of carbon (C) relations in trees under usual environmental conditions, including the distribution and turnover

of NSC reserves within both belowground and aboveground organs. This knowledge gap hinders our ability to predict how tree species will physiologically respond to stress and has broader implications for understanding C storage and cycling at the whole-tree and ecosystem levels.

Recent work quantified whole-tree NSC reserves and showed that the amount of NSCs stored differed between organs (Martínez-Vilalta et al. 2016, Smith et al. 2017, Furze et al. 2018*a*). However, the distribution and metabolic activity or availability of NSCs within individual organs (as indicated by seasonal fluctuation) is less understood. While previous studies have characterized within-organ NSC storage by measuring the radial patterns of NSC concentrations, particularly in the stemwood (Barbaroux and Bréda 2002, Hoch et al. 2003, Gérard and Bréda 2014, Zhang et al. 2014, Richardson et al. 2015, Smith et al. 2017), relatively few studies have measured the radial patterns of NSC age to assess the degree to which within-organ NSC storage represents a mix of older and newer NSCs (Richardson et al. 2015, Trumbore et al. 2015). When these radial patterns have been measured, it has often been in the stem sapwood only, for a single tree of a given species, or at a single point in time (Barbaroux and Bréda 2002, Richardson et al. 2015). Quantifying within-organ NSC dynamics throughout the entire organ, for diverse species, and on seasonal timescales is essential for determining whether reserves in deeper tissues become sequestered and metabolically unavailable (Millard et al. 2007).

The stem is a complex organ that not only provides infrastructure to the tree but also plays an important role in its overall C balance by storing a large proportion of NSC reserves (i.e., up to 40% of the NSC pool in temperate trees) (Richardson et al. 2015, Furze et al. 2018*b*). In the stemwood, NSC concentrations tend to decrease across the younger sapwood toward the sapwood–heartwood boundary and then remain constant throughout the heartwood to the pith (Hoch et al. 2003). However, high levels of NSCs have also been observed deep in the xylem (Würth et al. 2005, Smith et al. 2017). Furthermore, younger NSCs dominate the outermost growth rings of the stemwood, with limited 'mixing in' of younger NSCs to older growth rings (Richardson et al. 2015, Trumbore et al. 2015). Despite these efforts, how NSC age is distributed within belowground organs like coarse roots and, in general, how radial patterns of NSC concentrations within the stemwood vary across seasons and between species have largely been ignored due to sampling and cost limitations.

Of critical importance is the fact that the woody characteristics of the stem are not universal among species. Trees differ in their wood anatomy, which drives both their phenology and physiology, and in turn may influence NSC distribution, dynamics and availability. For example, ring-porous species initiate radial stem growth in the spring prior to leaf out using previously stored reserves, while diffuse-porous species do the opposite (Bréda and Granier 1996, Michelot et al. 2012, Panchen et al. 2014). Additionally, the distribution of xylem components differs based on wood anatomy. Ring-porous species have a functional sapwood zone that is distinguished from the deeper non-conductive heartwood; this boundary is less well-defined or absent in diffuse-porous species (Plavcová and Jansen 2015). Deeper stemwood reserves may be less dynamic, especially in older rings located in the heartwood (Spicer 2005).

To better understand within-organ NSC dynamics and reserve availability, we provide a detailed accounting of the spatial and temporal variation of NSCs within the stem of temperate trees with contrasting wood anatomy. We collected monthly stemwood samples from four species, divided these samples into radial segments from the cambium to the pith and measured their sugar and starch concentrations. This high-resolution sampling allows for the assessment of radial NSC patterns on seasonal timescales and in multiple species. In a subset of trees, we estimated the mean age of sugar within and between different organs. In general, we hypothesized that outer tissues would contain young, seasonally dynamic NSCs, while older NSCs would be less dynamic in deeper tissues. However, we expected the radial patterns of stemwood NSC concentrations as well as the degree of seasonal fluctuation within each radial segment to differ based on wood anatomy. Specifically, we hypothesized that NSCs would fluctuate across the seasons in deeper stemwood segments of diffuse-porous trees compared to ring-porous trees due to differences in the distribution of functional sapwood.

Materials and methods

Study site

Field sampling was conducted at Harvard Forest, an oak-dominated, mixed temperate forest located in Petersham, MA, USA (42.53°N, 72.17°W). We selected mature trees from the following five species for NSC concentration and/or radiocarbon analyses: red oak (*Quercus rubra* L.), white ash (*Fraxinus americana* L.), red maple (*Acer rubrum* L.), paper birch (*Betula papyrifera* Marshall) and American beech (*Fagus grandifolia* Ehrh). These trees represent the dominant species in the Prospect Hill Tract of Harvard Forest and differ in wood anatomy. Red oak and white ash are ring-porous species, whereas red maple, paper birch and American beech are diffuse-porous species.

Field collection

Monthly samples were collected from 18 trees along Prospect Hill Rd: two ring-porous species, red oak ($n = 6$) and white ash ($n = 3$), and two diffuse-porous species, red maple ($n = 6$) and paper birch ($n = 3$). Each month throughout 2014, a stemwood core to the pith was collected from each of these trees with a standard 4.3-mm increment borer (Haglöf Company Group,

Långsele, Sweden). The initial core was collected starting at breast height on the south or southwest side of each tree, and subsequent cores were collected in a zigzag pattern. Samples were kept on dry ice in the field during each collection and then stored at −80 °C until NSC analysis. Tree and stemwood characteristics were included in Table S1 available as Supplementary Data at *Tree Physiology* Online, including tree age, height, diameter at breast height (DBH), the approximate number of rings in each stemwood segment and the location of the sapwood–heartwood boundary.

In November 2015, we selected 12 trees for radiocarbon (^{14}C) analysis of bulk sugars: two ring-porous species, red oak ($n = 3$) and white ash ($n = 3$), and two diffuse-porous species, red maple ($n = 3$) and American beech ($n = 3$). Approximately half ($n = 7$) of these trees had also been sampled in 2014 for monthly stemwood NSC measurements. We sampled American beech for ^{14}C analysis instead of paper birch due to declining health of a previously sampled tree and the absence of an appropriate alternate within close proximity. A sunlit branch (ca 1–1.5 cm diameter, multi-year 3–5 years old), stemwood cores, coarse root cores and fine roots were collected from each tree and were kept on dry ice in the field and then stored at −80 °C until ^{14}C analysis. Tree characteristics were reported in Table S2 available as Supplementary Data at *Tree Physiology* Online.

Nonstructural carbohydrates analysis

Stemwood cores collected monthly throughout 2014 were subdivided into segments from the cambium (designated as 0) to the pith to determine the radial distribution of sugar and starch concentrations. Stemwood cores were divided into six segments after the bark and phloem were removed with a razor blade under a dissecting microscope: 0–1, 1–2, 2–3, 3–4, 4–8 and 8 cm-pith. Based on ring widths from January 2014 stemwood cores, we estimated the size of the 8 cm-pith segment by summing the ring widths to the pith and subtracting 8 cm. The average size of the 8 cm-pith segment was 8.1 cm (±3.8 SD, $n = 9$) for ring-porous trees and 6.5 cm (±2.1 SD, $n = 9$) for diffuse-porous trees. A coarser estimate of the size of the 8 cm-pith segment can also be obtained using DBH measurements, yielding 10.1 cm (±3.4 SD, $n = 9$) for ring-porous trees and 8.1 cm (±2.6 SD, $n = 9$) for diffuse-porous trees.

Segmented samples were freeze-dried (FreeZone 2.5, Labconco, Kansas City, MO, USA, and Hybrid Vacuum Pump, Vacuubrand, Wertheim, Germany) and ground (mesh 20, Thomas Scientific Wiley Mill, Swedesboro, NJ, USA; SPEX SamplePrep 1600 MiniG, Metuchen, NJ, USA). Sugar and starch concentrations were measured for all stemwood segments collected monthly throughout 2014 with the exception of the deepest heartwood (8 cm-pith); this region was only measured in January and July 2014. Since the NSC concentrations were similar between these 2 months, the 8 cm-pith segment of the remaining months of the year was not analyzed. Instead, we rely on imputed estimates to fill in the gaps for the missing data for the 8 cm-pith segment (see Data analysis).

To measure sugar concentrations (adapted from Chow and Landhäusser 2004), 10 mg of stem tissue was freeze-dried and then extracted three times with 80% ethanol in a 90 °C water bath for 10 min, followed by colorimetric analysis with phenol–sulfuric acid. The sugar extract was read at 490 nm on a spectrophotometer (Epoch Microplate Spectrophotometer, Bio-Tek Instruments, Winooski, VT or Thermo Fischer Scientific GENESYS 10S UV-Vis, Waltham, MA, USA). Sugar concentrations (expressed as mg sugar per g dry wood) were calculated from a 1:1:1 glucose–fructose–galactose (Sigma Chemicals, St. Louis, MO) standard curve. This gives an estimate of total soluble sugars in the sample.

To determine starch concentrations, the remaining stem tissue was solubilized in 0.1 N sodium hydroxide and neutralized with 0.1 N acetic acid and then digested with an α-amylase/amyloglucosidase digestive enzyme solution in sodium acetate buffer (0.05 M, pH 5.1) for 24 h. Glucose hydrolysate was determined using a peroxidase–glucose oxidase–color reagent solution (Sigma Chemicals, St Louis, MO, USA) and read at 525 nm. Starch concentrations (expressed as mg starch per g dry wood) were calculated based on a glucose (Sigma Chemicals) standard curve. Sugar and starch concentrations were then summed to obtain total NSC concentrations for each sample. When conducting NSC analyses, we included at least one internal laboratory standard (red oak stemwood, Harvard Forest, Petersham, MA, USA) per analysis. The uncertainty in NSC concentration measurements is reported in Methods S1 available as Supplementary Data at *Tree Physiology* Online.

Radiocarbon (^{14}C) analysis

We used the ^{14}C 'bomb spike' to estimate the mean age of sugars within and between different organs sampled in November 2015. The cost of conducting ^{14}C analyses precluded the measurement of starch and additional tissues like deeper organ segments, so we focused on radial patterns of sugars in the outer 2 cm of stemwood and coarse roots where we expected sugars to be the most dynamic (Richardson et al. 2013, 2015). These organs were subdivided into four segments starting from the cambium: 0–0.5, 0.5–1, 1–1.5 and 1.5–2 cm. In addition to quantifying these radial patterns in the stemwood and coarse roots, the mean age of sugars was also determined in multi-year sunlit branches and bulk fine roots to compare between organs.

For ^{14}C analysis, soluble C was extracted by hot water, combusted to CO_2, purified on a vacuum line, converted to graphite and then analyzed for ^{14}C content at the W.M. Keck Carbon Cycle Accelerator Mass Spectrometry facility at the University of California, Irvine (Xu et al. 2007, Beverly et al. 2010, Czimczik et al. 2014). The analytical uncertainty for ^{14}C is about

0.003 fraction modern for modern samples based on long-term measurements of secondary standards. ^{14}C content was then directly compared to the Northern Hemisphere atmospheric $^{14}CO_2$ record (Levin et al. 2008; X.Xu, unpublished results) to estimate the mean age of C in the sugars in the sample (or sugar mean age).

The background air at Harvard Forest has been previously shown to be consistent with the atmospheric record (Carbone et al. 2013, Richardson et al. 2013). To confirm, we collected the annual plant jewelweed (*Impatiens capensis* Meerb) at Harvard Forest to quantify background atmospheric $^{14}CO_2$ and the signature of current year photoassimilates at the time of sampling. Annual jewelweed samples were collected and processed for ^{14}C content each year from 2011 to 2015, which includes our study years 2014–15 (Table S3 available as Supplementary Data at *Tree Physiology* Online). The uncertainty in ^{14}C measurements as well as limitations of the sugar extraction is reported in Methods S1 available as Supplementary Data at *Tree Physiology* Online.

Data analysis

We estimated the effects of segment depth (i.e., 0–1, 1–2, 2–3, 3–4, 4–8 and 8 cm-pith) on total NSC, sugar and starch concentrations for both ring-porous and diffuse-porous trees using Bayesian hierarchical models with the brms package (Bürkner 2017), version 2.3.1, in R (R Development Core Team 2017). Monthly stemwood NSC concentrations from 2014 were categorized by season (winter = January, February; spring = March, April, May; summer = June, July, August; autumn = September, October, November). Due to missing data for the 8 cm-pith segment, we imputed data for the missing months based on actual values measured in January and July (Gelman and Hill 2006). Seasons were modeled hierarchically, generating an estimate of the overall response across season and estimates of season-level responses—and the posterior distributions from which they were drawn. The intercept in the model was segment 0–1 cm since the predictors were discrete groups:

$$\begin{aligned} y_i = {} & \alpha_{\text{season}[i]} + \beta_{\text{segment1-2}_{\text{season}[i]}} + \beta_{\text{segment2-3}_{\text{season}[i]}} \\ & + \beta_{\text{segment3-4}_{\text{season}[i]}} + \beta_{\text{segment4-8}_{\text{season}[i]}} \\ & + \beta_{\text{segment8-pith}_{\text{season}[i]}} + \varepsilon_i, \end{aligned}$$

$$\varepsilon_i \sim N\left(0, \sigma_y^2\right) \quad (1)$$

The α and each of the five β coefficients were modeled at the season level, as follows:

$$\alpha_{\text{season}} \sim N\left(\mu_\alpha, \sigma_\alpha\right)$$

$$\beta_{\text{segment1-2}_{\text{season}}} \sim N\left(\mu_{\text{segment1-2}}, \sigma_{\text{segment1-2}}\right) \quad (2)$$

$$\beta_{\text{segment2-3}_{\text{season}}} \sim N\left(\mu_{\text{segment2-3}}, \sigma_{\text{segment2-3}}\right)$$

$$\beta_{\text{segment3-4}_{\text{season}}} \sim N\left(\mu_{\text{segment3-4}}, \sigma_{\text{segment3-4}}\right)$$

$$\beta_{\text{segment4-8}_{\text{season}}} \sim N\left(\mu_{\text{segment4-8}}, \sigma_{\text{segment4-8}}\right)$$

$$\beta_{\text{segment8-pith}_{\text{season}}} \sim N\left(\mu_{\text{segment8-pith}}, \sigma_{\text{segment8-pith}}\right)$$

where *i* represents each unique observation; season is the season; α represents the intercept, which is again segment 0–1 cm; β terms represent slope estimates and *y* is the total, sugar or starch concentration. We additionally estimated the effects of organ on the sugar mean age using a Bayesian model, where branch was the intercept since, again, the predictors were discrete groups:

$$\begin{aligned} y_i = {} & \alpha_{[i]} + \beta_{\text{stemwood0-0.5}_{[i]}} + \beta_{\text{stemwood0.5-1}_{[i]}} \\ & + \beta_{\text{stemwood1-1.5}_{[i]}} + \beta_{\text{stemwood1.5-2}_{[i]}} + \beta_{\text{coarseroot0-0.5}_{[i]}} \\ & + \beta_{\text{coarseroot0.5-1}_{[i]}} + \beta_{\text{coarseroot1-1.5}_{[i]}} + \beta_{\text{coarseroot1.5-2}_{[i]}} \\ & + \beta_{\text{fineroot}_{[i]}} + \varepsilon_i, \end{aligned}$$

$$\varepsilon_i \sim N\left(0, \sigma_y^2\right) \quad (3)$$

We ran four chains, each with 2500 warm-up iterations and 4000 sampling iterations for a total of 6000 posterior samples for each predictor for each model using weakly informative priors. Increasing priors threefold did not impact our results. We evaluated our model performance based on $\hat{R}$ values that were close to one. We also evaluated high effective sample size, n_{eff} (4000 for most parameters, but as low as 794 for a few parameters in the diffuse-porous sugar concentration model). We additionally assessed chain convergence and posterior predictive checks visually (Gelman et al. 2014).

Figures 1–3 present model estimates generated using the above Bayesian hierarchical modeling approach. These model estimates for total NSC, sugar and starch concentrations in ring-porous trees (Tables S4–S6 available as Supplementary Data at *Tree Physiology* Online) and diffuse-porous trees (Tables S7–S9 available as Supplementary Data at *Tree Physiology* Online), as well as model estimates for sugar mean age (Tables S10 and S11 available as Supplementary Data at *Tree Physiology* Online), are provided. Additionally, we display measured total NSC, sugar and starch concentrations in ring-porous trees and diffuse-porous trees along with analysis of variance results for stemwood sugar dynamics to aid interpretation (Figure S1 available as Supplementary Data at *Tree Physiology* Online). A comparison between measured and predicted concentrations is provided in Figure S2 available as Supplementary Data at *Tree Physiology* Online.

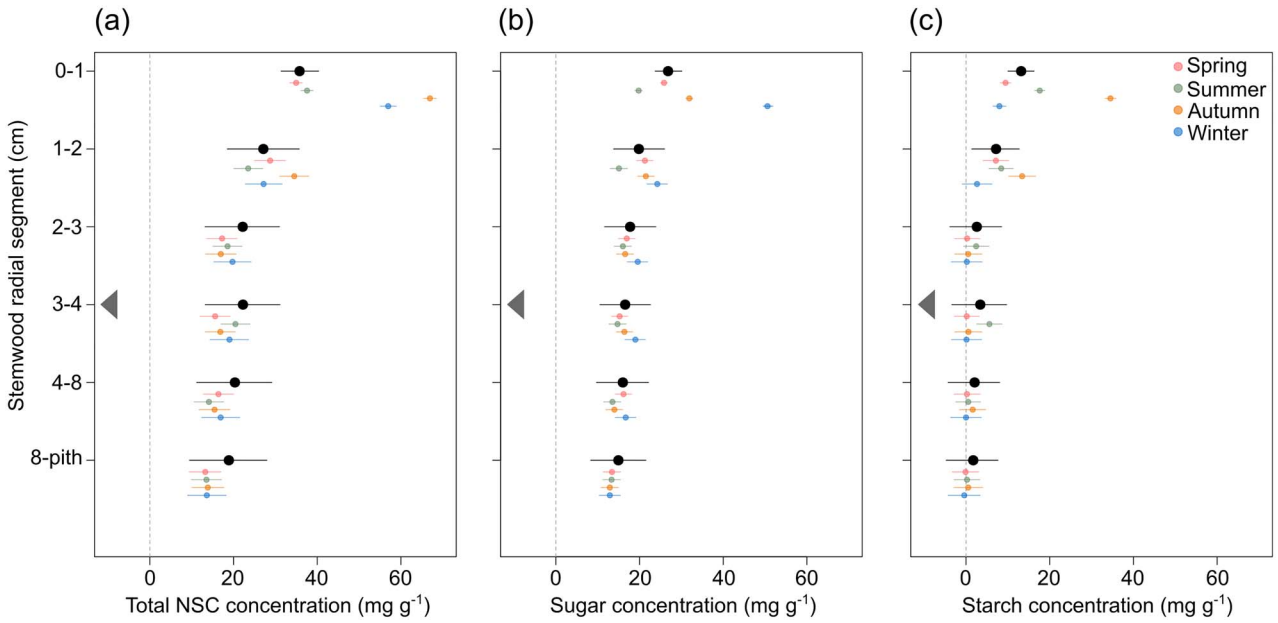

Figure 1. Radial patterns of (a) total NSC, (b) sugar and (c) starch concentrations in the stemwood of ring-porous trees sampled throughout 2014. Stemwood radial segments (cm) were sampled from just inside the removed bark at the cambium (0–1 cm) and continued to the pith (8 cm-pith). The gray triangle indicates the average stemwood segment in which the heartwood began for ring-porous trees (Table S1 available as Supplementary Data at *Tree Physiology* Online). Large black circles indicate model estimated mean annual concentrations, while smaller colored circles indicate model estimated mean concentrations for each season. Error bars denote the 50% uncertainty interval of each model estimated mean. Models were run independently such that the model estimates in (a) are not the sum of (b) and (c). Modeling results are presented in Tables S4–S6 available as Supplementary Data at *Tree Physiology* Online. In (c), some error bars extend below 0 mg g^{-1} for mean model estimates of starch, and we caution that negative values are not biologically realistic. In these cases, the model is generating estimates based on measured starch concentrations that were very low or zero. Corresponding figures displaying the measured total NSC, sugar and starch concentrations are presented in Figure S1 available as Supplementary Data at *Tree Physiology* Online.

Data, model code and output are available on GitHub at github.com/cchambe12/nscradiocarbon. Measured NSC concentrations and sugar mean ages from this project are also available on the Harvard Forest Data Archive (Furze 2020*a*, 2020*b*). The measured ^{14}C data are also reported in Table S12 available as Supplementary Data at *Tree Physiology* Online.

Results

Radial patterns of stemwood NSC concentrations

In the stemwood, total NSC concentrations were the highest near the cambium, declined radially across the outermost segments and then remained consistent to the pith (Figures 1a and 2a; Tables S4 and S7 available as Supplementary Data at *Tree Physiology* Online). Nearest the cambium, mean annual total NSC concentrations were 35.8 mg g^{-1} (±7.4 SD) and 25.4 mg g^{-1} (±6.3 SD) in ring-porous and diffuse-porous trees, respectively. In general, sugar concentrations were highest in the winter (ring-porous 50.6 mg g^{-1} (±5.4 SD); diffuse-porous 23.1 mg g^{-1} (±4.2 SD)), and starch concentrations were highest in the summer/autumn (ring-porous 34.5 mg g^{-1} (±5.8 SD); diffuse-porous 46.2 mg g^{-1} (±6.4 SD)), particularly in the outermost segment (Figures 1b and c and 2b and c). However, the distribution of sugars and starch across radial segments as well as the degree of seasonal fluctuation within segments differed based on wood anatomy.

Radial patterns of stemwood sugar concentrations in ring-porous versus diffuse-porous trees

In the ring-porous trees, sugar concentrations generally declined over the outer 2 cm of stemwood and remained consistent to the pith regardless of season (Figure 1b; Table S5 available as Supplementary Data at *Tree Physiology* Online). The decline was most pronounced in the winter, with sugar concentration decreasing by ~50% between the outer two stemwood segments (0–1 and 1–2 cm) (Figure 1b). In contrast, in diffuse-porous trees, sugar concentrations were relatively stable from the cambium to the pith regardless of season (Figure 2b; Table S8 available as Supplementary Data at *Tree Physiology* Online). For both wood anatomies, sugar concentrations were the highest during the winter and the lowest during the summer in all radial segments, with the exception of the deepest segment where sugar concentrations did not fluctuate across the seasons (Figures 1b and 2b).

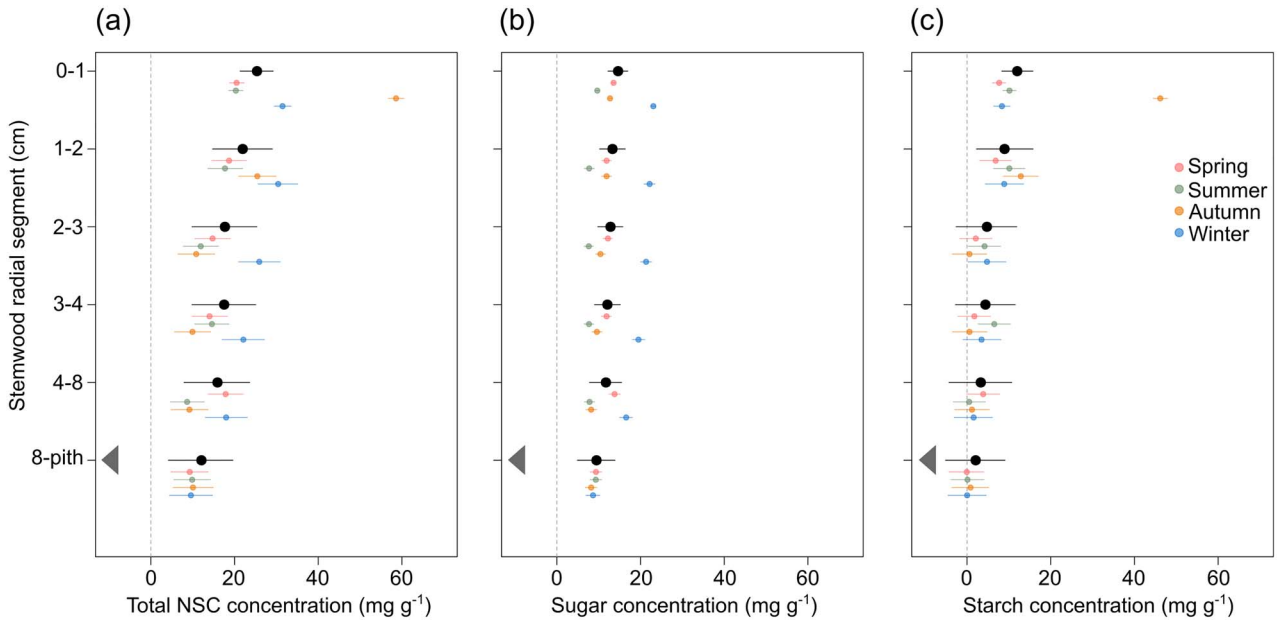

Figure 2. Radial patterns of (a) total NSC, (b) sugar and (c) starch concentrations in the stemwood of diffuse-porous trees sampled throughout 2014. Stemwood radial segments (cm) were sampled from just inside the removed bark at the cambium (0–1 cm) and continued to the pith (8 cm-pith). The gray triangle indicates the average stemwood segment in which the heartwood begins for diffuse-porous trees (Table S1 available as Supplementary Data at *Tree Physiology* Online). Large black circles indicate model estimated mean annual concentrations, while smaller colored circles indicate model estimated mean concentrations for each season. Error bars denote the 50% uncertainty interval of each model estimated mean. Models were run independently such that the model estimates in (a) are not the sum of (b) and (c). Modeling results are presented in Tables S7–S9 available as Supplementary Data at *Tree Physiology* Online. In (c), some error bars extend below 0 mg g^{-1} for mean model estimates of starch, and we caution that negative values are not biologically realistic. In these cases, the model is generating estimates based on measured starch concentrations that were very low or zero. Corresponding figures displaying the measured total NSC, sugar and starch concentrations are presented in Figure S1 available as Supplementary Data at *Tree Physiology* Online.

Radial patterns of stemwood starch concentrations in ring-porous versus diffuse-porous trees

The radial patterns of starch concentrations in the stemwood were more consistent between trees with different wood anatomies than were sugar concentrations. Starch concentrations were the highest near the cambium, declined over the outer segments and then remained constant to the pith with little or no starch present (Figures 1c and 2c; Tables S6 and S9 available as Supplementary Data at *Tree Physiology* Online). The decline was most pronounced in autumn, when starch concentrations decreased by ~60 and 70% between the outer two stemwood segments (0–1 and 1–2 cm) in ring-porous and diffuse-porous trees, respectively. Due to low starch levels beyond the outermost stemwood segments across seasons, sugars dominated deeper stemwood tissues.

Seasonal fluctuation within stemwood radial segments in ring-porous versus diffuse-porous trees

To understand how NSC concentrations fluctuated across the seasons, we identified the mean for each season and compared the mean minimum NSC concentration to the mean maximum NSC concentration in each stemwood segment to quantify the degree of fluctuation throughout the year. This seasonal fluctuation in a given segment is indicative of metabolic activity/availability (i.e., the use and exchange of NSCs) at that depth in the stem and is best exemplified by the fluctuation of sugar concentrations, since sugars were high throughout the entire stemwood and play an established role in metabolism and transport.

In both ring-porous and diffuse-porous trees, sugar concentrations decreased between the spring and summer and then increased through the winter in each stemwood segment (Figures 1b and 2b). Seasonal variation was greatest in the outermost stemwood segment (0–1 cm), fluctuating by nearly 150% for trees of both wood anatomies (Figures 1b and 2b). However, the seasonal fluctuation of sugar concentrations in deeper radial segments differed based on wood anatomy.

Seasonal fluctuation remained high across stemwood segments for diffuse-porous trees (Figure 2b). Moving across segments from the cambium to the 4–8 cm segment, the seasonal fluctuation was 138, 187, 179, 154 and 112%. In contrast, the seasonal fluctuation was dampened when moving radially toward the pith in the ring-porous trees, declining by 85% between the 0–1 cm segment and the 4–8 cm segment (Figure 1b); the seasonal fluctuation was 156, 61, 22, 29 and 23%. In all trees, sugar concentrations did not vary across the seasons in the deepest stemwood segment (8 cm-pith).

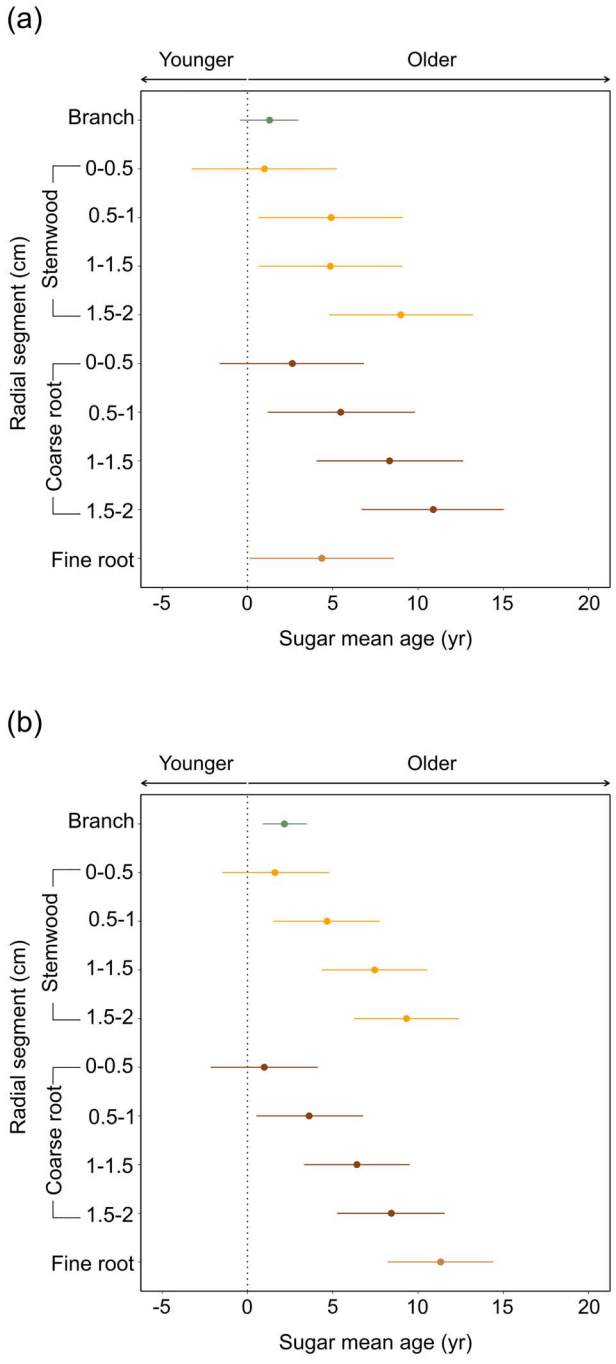

Figure 3. Mean age of sugar interpreted from radiocarbon (^{14}C) content of extracted sugars from radial segments of stemwood and coarse roots as well as bulk branches and fine roots of (a) ring-porous and (b) diffuse-porous trees. Radial measurements were taken in 0.5 cm segments for stemwood and coarse roots, with the first segment (0–0.5 cm) taken just inside the removed bark at the cambium and continuing across the outer 2 cm to the deepest segment (1.5–2 cm). Symbols indicate model estimated mean sugar mean age. Error bars denote the 50% uncertainty interval of each model estimated mean. Modeling results are presented in Tables S10 and S11 available as Supplementary Data at *Tree Physiology* Online. Error bars extending below 0 years for mean model estimates of sugar mean age are not biologically realistic. Measured sugar mean ages are provided in Table S12 available as Supplementary Data at *Tree Physiology* Online.

Furthermore, the location of the sapwood–heartwood boundary differed between trees. Ring-porous trees generally had shallower (3.7 cm ± 3.1 SD, $n = 9$) sapwood–heartwood transition zones than diffuse-porous trees (9.3 cm ± 2.6 SD, $n = 7$; $t(14) = -3.94$, $P < 0.01$); this boundary could not be identified for two diffuse-porous trees and was excluded from the calculation, likely yielding an underestimate for the depth of the sapwood–heartwood transition in diffuse-porous trees (Table S1 available as Supplementary Data at *Tree Physiology* Online). In line with the above differences in functional sapwood area, (i) sugar concentrations declined over the outer 2 cm and remained consistent to the pith for ring-porous trees, while sugar concentrations remained high and fairly stable across segments for diffuse-porous trees and (ii) the seasonal fluctuation of sugar concentrations was greater in deeper stemwood segments for diffuse-porous trees compared with ring-porous trees.

Radial patterns of sugar mean age and differences between organs

The mean age of sugar varied radially within organs and also differed between organs (Figure 3). Within the stemwood and coarse roots, the sugar mean age increased radially across the outer 2 cm from the cambium toward the pith in both ring-porous (Figure 3a; Table S10 available as Supplementary Data at *Tree Physiology* Online) and diffuse-porous trees (Figure 3b; Table S11 available as Supplementary Data at *Tree Physiology* Online). In the outermost segment (0–0.5 cm) of both organs, sugars were very young (<5 years), while in the deepest segment (1.5–2 cm) measured, sugars were nearly a decade old. Notably, the oldest measured sugar mean age in this study was 32.5 years in deeper coarse root segments (1–1.5 cm/1.5–2 cm) of a ring-porous red oak tree (Table S12 available as Supplementary Data at *Tree Physiology* Online).

When comparing between organs, branch sugar mean age was in line with recent photosynthetic products (ca 1–2 years), while fine root sugars varied in age. Ring-porous fine root sugars (4.3 years (±3.9 SD)) were nearly three times younger than in diffuse-porous trees (11.3 years ± (2.7 SD)) (Figure 3; Tables S10 and S11 available as Supplementary Data at *Tree Physiology* Online). Measured sugar mean age was negatively correlated with the age of the tree from which it was extracted for fine roots ($r = -0.61$, $P = 0.04$; further discussed in Figure S3 available as Supplementary Data at *Tree Physiology* Online).

Discussion

By resolving the radial patterns in the concentration of NSCs within the stemwood on seasonal timescales, our results provide insight into the dynamics of NSC reserves and their use for proper tree function under usual environment conditions.

The seasonal fluctuation of NSCs in the stemwood is characteristic of temperate deciduous trees, which face asynchrony in photosynthetic supply and metabolic demand (Carbone et al. 2013, Richardson et al. 2013). On a finer scale, the wood anatomy of the stem adds a layer of complexity as the proportion of functional cells as well as the arrangement of vessels differs between species (Morris et al. 2016). Living ray and axial parenchyma in the sapwood region impose a boundary for NSC storage, and the cellular processes that occur within them may influence stemwood NSC dynamics (Plavcová and Jansen 2015, Plavcová et al. 2016); these metabolic activities involving the use and exchange of NSCs include processes like radial and axial transport, sugar utilization (i.e., respiration, biomass) and sugar–starch interconversions (i.e., conversion to sugar maintains and recovers hydraulic conductivity; Klein et al. 2018).

We hypothesized that the contrasting wood anatomies of ring-porous and diffuse-porous trees would relate to the radial distribution of stemwood NSC concentrations. Previous studies have identified a sharp decline in NSC concentrations with increasing sapwood depth in ring-porous oak compared with a more gradual decline in diffuse-porous species (Barbaroux and Bréda 2002, Hoch et al. 2003), and more generally, NSC concentrations tend to decline with ring age/depth in both deciduous and coniferous species (Terziev et al. 1997, Hoch et al. 2003, Richardson et al. 2015). While the patterns of radial starch distribution were similar between wood anatomies (Figures 1c and 2c), we found that sugar concentrations declined rapidly across the outer segments and then remained constant to the pith for ring-porous trees (Figure 1b), whereas sugar concentrations were more stable across all stemwood segments for diffuse-porous trees (Figure 2b), thus, providing support for our hypothesis. Interestingly, these radial patterns were consistent across seasons, which reinforce the idea that NSC dynamics may operate within the limits set forth by the physical structure and metabolic function of wood (Plavcová and Jansen 2015); that is, while parenchyma fractions may not limit storage capacity (Godfrey et al. 2020), they may constrain the spatial distribution and utilization of NSCs.

Furthermore, we expected wood anatomy to play an important role in NSC dynamics and availability by influencing the seasonal fluctuation of NSC concentrations within radial stemwood segments when moving from the cambium to the pith. Specifically, we hypothesized that NSCs would fluctuate across the seasons in deeper stemwood segments of diffuse-porous trees compared with ring-porous trees. Sugars were highly dynamic in the outermost stemwood segments, but, while this seasonal fluctuation declined in deeper segments for ring-porous trees (Figure 1b), it remained high for diffuse-porous trees (Figure 2b). Thus, greater and deeper fluctuation was evident in diffuse-porous trees in line with their larger functional sapwood area in the stem.

While the living parenchyma within the functional sapwood serve as boundaries for NSC dynamics, additional consideration should be given to the water transport capacity of temperate trees. Vessels are narrow and evenly distributed within the annual growth rings of diffuse-porous trees, whereas the growth rings have wide earlywood vessels and narrow latewood vessels in ring-porous trees (Taneda and Sperry 2008). The wide earlywood vessels are vulnerable to freeze-induced embolism, leaving only the most recent growth rings functional for water transport (Zimmermann 1983, Ellmore and Ewers 1986). Because C and water dynamics are intimately tied in plants, the higher seasonal fluctuation of sugars in deeper segments of diffuse-porous trees may be linked to functional xylem vessels. Further, recent work showed that diffuse-porous red maple trees were able to transport water across growth rings through intervessel connections (Wason et al. 2019), which begs the question of whether these cross-ring intervessel connections could provide a pathway for NSCs as well.

A characteristic of heartwood formation is parenchyma cell death (Spicer 2005). Most, if not all, of the deepest segment at the stem center (8 cm-pith segment) was within the heartwood of our study trees and NSCs did not vary across the seasons in this segment (Figures 1 and 2). This finding supports our expectation that NSCs would exhibit less seasonal fluctuation in deeper stemwood tissues, especially in segments residing within the inactive heartwood region where NSCs may also be metabolically unavailable (Stewart 1966). Yet, we recommend caution when interpreting the observed lack of seasonal fluctuation of NSCs in this segment. First, NSC concentrations in the 8 cm-pith segment were only measured in the summer and winter; thus, we acknowledge that our model estimates for the spring and autumn for this segment may not accurately represent tree physiology and any seasonal fluctuation that may occur at the stem center. Second, while NSCs in the 8 cm-pith segment were not metabolically active since they did not fluctuate across the seasons in the year of our study, this does not imply that NSCs in the 8 cm-pith segment are metabolically unavailable. It is plausible that these deeper reserves are metabolically available and used by trees on interannual timescales, whether naturally or in response to stress (Gessler and Treydte 2016).

Despite a lack of seasonal fluctuation near the pith, sugars varied throughout the year in the next deepest segment (4–8 cm). While the seasonal fluctuation was particularly evident in diffuse-porous trees (Figure 2b), seasonal fluctuation was also observed in ring-porous trees, but to a far lesser degree (nearly 5 times less; Figure 1b). This difference may be explained by the fact that, in most cases, the 4–8 cm segment resided fully within the sapwood for diffuse-porous trees and within the heartwood for ring-porous trees. Assuming the weaker seasonal fluctuation of sugars in the heartwood-bound 4–8 cm segment of ring-porous trees represents metabolic activity, then it raises the question of whether metabolically active,

NSC-containing ray parenchyma can extend and persist beyond the sapwood–heartwood boundary.

The heartwood is typically identified by color, but there is some evidence that this color change occurs before the processes associated with heartwood formation, like ray parenchyma death, have taken place (Nobuchi et al. 1984). Further, at least in conifer species, the heartwood region is not uniform along the entire stem (Stokes and Berthier 2000, Tulik et al. 2019). Thus, the duration of heartwood development, its distribution along the stem and the longevity of parenchyma cells throughout the stem could influence measured NSC dynamics. Future work should combine the quantification of NSC dynamics with the staining of living/dead parenchyma as well as functional/nonfunctional wood fractions to further resolve the availability of NSC reserves in deeper stemwood tissues.

Sugars in the outermost segment nearest the cambium were not only the most dynamic, but when considering the radial patterns of sugar mean age within the stemwood, they were also the youngest (Figure 3). This finding supports sapwood–phloem exchange and the preferential use of younger, shallower NSCs for growth and metabolism (Frey-Wyssling and Bosshard 1959, Ziegler 1964, Lacointe et al. 1993). Sugar age increased across radial segments when moving toward the pith, regardless of wood anatomy, and was consistent between stemwood and coarse roots. The age in the deepest stemwood segment (1.5–2 cm) was 8.9 (±3.8 SD) and 9.3 (±2.7 SD) for ring-porous and diffuse-porous species, respectively, and corresponded to older growth rings (ca ≥10 years). Assuming this radial trend continues and sugar age increases in older growth rings as has been previously reported for other temperate tree species (Richardson et al. 2015), we would then expect the seasonally dynamic sugars in deeper segments (i.e., 4–8 cm; Figures 1b and 2b) to be older, possibly decades old. These metabolically available, deeper and likely older stemwood reserves would support previous radiocarbon signatures of NSCs and CO_2 efflux, which indicate that decades-old reserves contribute to growth and respiration in both stem and roots (Carbone et al. 2013, Muhr et al. 2013, Trumbore et al. 2015).

Due to cost limitations, we were not able to measure sugar age in deeper stemwood segments beyond the outer 2 cm, and we acknowledge this as a limitation of our study. Future progress in this area should examine the seasonal dynamics and age of both sugars and starch, particularly in deeper segments, and explore reserve age, annual ring age and segment depth as drivers of NSC availability. While we showed that the radial patterns of sugar mean age were consistent between wood anatomies in the outer 2 cm of stemwood (Figure 3), this pattern may differ in deeper segments where we found the seasonal fluctuation of sugars to be greater for diffuse-porous trees. This greater and deeper fluctuation may influence the mixing of young and old sugars across stemwood segments as well as their availability to support metabolic functions. Additionally, to further resolve the storage and availability of NSC reserves in the stem, consideration should be given to the emerging idea that NSCs may appear older than they actually are due to refixation of respired CO_2 in tree stems (Bloemen et al. 2013, Hilman et al. 2019).

Moreover, our measurement of sugar age in both aboveground and belowground organs allows for a more comprehensive understanding of whole-tree NSC storage and utilization (Figure 3). Aboveground, young sugars (1–2 years) were found in the branches. These younger NSCs likely resulted from fast turnover rates and/or refilling of branch reserves with current year photoassimilates following leaf out (Schädel et al. 2009, Epron et al. 2012). Belowground, older sugars were measured in deeper coarse root segments and fine roots, which is in agreement with previous reports of older C stored in the root system and used to fuel root respiration (Czimczik et al. 2006, Schuur and Trumbore 2006, Richardson et al. 2015). Overall, moving vertically from the canopy to the root system and moving radially from the cambium to the pith, sugars become older and less seasonally dynamic, with wood anatomy driving stemwood dynamics.

Conclusions

By using repeat within-organ sampling and radiocarbon methods, our work provides insight into the radial distribution of the concentration and age of NSCs within trees with contrasting wood anatomy and how these patterns contribute to the overall whole-tree NSC pool. Notably, our assessment of sugar concentrations across radial stemwood segments on seasonal timescales provides an indicator of metabolic availability and suggests that while deeper, and likely older, reserves in the stemwood fluctuate across the seasons, the deepest stemwood reserves were not used by temperate trees under usual environmental conditions. The use of these deep reserves should be further explored in the context of climatic variations (i.e., interannual times, drought) to advance our understanding of tree C physiology and cycling.

Supplementary Data

Supplementary Data for this article are available at *Tree Physiology* Online.

Authors' contribution

M.E.F., B.A.H., M.S.C. and A.D.R. planned the project. M.E.F., B.A.H. and D.M.A. conducted the field sampling. M.M.W. conducted dendrochronological analysis and contributed to sample preparation. B.A.H. contributed to dendrochronological analysis. M.E.F. conducted NSC analyses. M.E.F. conducted radiocarbon

extractions and analysis with guidance from J.C.W., X.X., C.I.C. and M.S.C. C.J.C. performed the data analyses. M.E.F. interpreted the results with contributions from A.D.R. M.E.F. took the lead in writing the manuscript, with feedback and approval from co-authors.

Acknowledgments

This work was supported by the National Science Foundation Graduate Research Fellowship under Grant No. DGE1144152. A.D.R. acknowledges additional support for research at Harvard Forest from the National Science Foundation's LTER program (DEB-1237491). This material is based upon work supported by the US Department of Energy, Office of Science, Office of Biological and Environmental Research.

References

Barbaroux C, Bréda N (2002) Contrasting distribution and seasonal dynamics of carbohydrate reserves in stem wood of adult ring-porous sessile oak and diffuse-porous beech trees. Tree Physiol 22:1201–1210.

Beverly RK, Beaumont W, Tauz D, Ormsby KM, von Reden KF, Santos GM, Southon JR (2010) The Keck Carbon Cycle AMS Laboratory, University of California, Irvine: status report. Radiocarbon 52:301–309.

Bloemen J, Mcguire MA, Aubrey DP, Teskey RO, Steppe K (2013) Transport of root-respired CO_2 via the transpiration stream affects aboveground carbon assimilation and CO_2 efflux in trees. New Phytol 197:555–565.

Bréda N, Granier A (1996) Intra- and interannual variations of transpiration, leaf area index and radial growth of a sessile oak stand (*Quercus petraea*). Ann For Sci 53:521–536.

Bürkner PC (2017) brms: an R package for Bayesian multilevel models using Stan. J Stat Softw 80:1–28.

Carbone MS, Czimczik CI, Keenan TF, Murakami PF, Pederson N, Schaberg PG, Xu X, Richardson AD (2013) Age, allocation and availability of nonstructural carbon in mature red maple trees. New Phytol 200:1145–1155.

Chow PS, Landhäusser SM (2004) A method for routine measurements of total sugar and starch content in woody plant tissues. Tree Physiol 24:1129–1136.

Czimczik CI, Trumbore SE, Carbone MS, Winston GC (2006) Changing sources of soil respiration with time since fire in a boreal forest. Glob Chang Biol 12:957–971.

Czimczik CI, Trumbore SE, Xu XM, Carbone MS, Richardson AD (2014) Extraction of nonstructural carbon and cellulose from wood for radiocarbon analysis. Bio Protoc 4:e1169.

Dietze MC, Sala A, Carbone MS, Czimczik CI, Mantooth JA, Richardson AD, Vargas R (2014) Nonstructural carbon in woody plants. Annu Rev Plant Biol 65:667–687.

Ellmore G, Ewers F (1986) Fluid flow in the outermost xylem increment of a ring-porous tree, *Ulmus americana*. Am J Bot 73:1771–1774.

Epron D, Bahn M, Derrien D et al. (2012) Pulse-labelling trees to study carbon allocation dynamics: a review of methods, current knowledge and future prospects. Tree Physiol 32:776–798.

Frey-Wyssling A, Bosshard HH (1959) Cytology of the ray cells in sapwood and heartwood. Holzforschung 13:129–137.

Furze M (2020*a*) Whole-tree nonstructural carbohydrate budgets in five species at Harvard Forest 2014. Harvard Forest Data Archive, HF308.

Furze M (2020*b*) Age of nonstructural carbohydrates in four tree species at Harvard Forest 2015. Harvard Forest Data Archive, HF341.

Furze ME, Huggett BA, Aubrecht DM, Stolz CD, Carbone MS, Richardson AD (2018*a*) Whole-tree nonstructural carbohydrate storage and seasonal dynamics in five temperate species. New Phytol 221:1466–1477.

Furze ME, Trumbore S, Hartmann H (2018*b*) Detours on the phloem sugar highway: stem carbon storage and remobilization. Curr Opin Plant Biol 43:89–95.

Gelman A, Hill J (2006) Data Analysis using regression and multilevel/hierarchical models. Cambridge University Press, New York, NY, USA.

Gelman A, Carlin J, Stern H, Dunson D, Vehtari A, Rubin D (2014) Bayesian data analysis, 3rd edn. CRC Press, Boca Raton, FL, USA.

Gérard B, Bréda N (2014) Radial distribution of carbohydrate reserves in the trunk of declining European beech trees (*Fagus sylvatica* L.). Ann For Sci 71:675–682.

Gessler A, Treydte K (2016) The fate and age of carbon - insights into the storage and remobilization dynamics in trees. New Phytol 209:1338–1340.

Godfrey JM, Riggio J, Orozco J, Guzmán-Delgado P, Chin ARO, Zwieniecki MA (2020) Ray fractions and carbohydrate dynamics of tree species along a 2750 m elevation gradient indicate climate response, not spatial storage limitation. New Phytol 225: 2314–2330.

Hartmann H, Trumbore S (2016) Understanding the roles of nonstructural carbohydrates in forest trees - from what we can measure to what we want to know. New Phytol 211:386–403.

Hilman B, Muhr J, Trumbore SE, Carbone MS, Yuval P, Joseph S (2019) Comparison of CO_2 and O_2 fluxes demonstrate retention of respired CO_2 in tree stems from a range of tree species. Biogeosciences 16:177–191.

Hoch G, Richter A, Körner C (2003) Non-structural carbon compounds in temperate forest trees. Plant Cell Environ 26:1067–1081.

Klein T, Zeppel MJB, Anderegg WRL, et al. (2018) Xylem embolism refilling and resilience against drought-induced mortality in woody plants: processes and trade-offs. Ecol Res 33:839–855.

Lacointe A, Kajji A, Daudet FA, Archer P, Frossard JS, Saint-Joanis B, Vandame M (1993) Mobilization of carbon reserves in young walnut trees. Acta Bot Gall 140:435–441.

Levin I, Hammer S, Kromer B, Meinhardt F (2008) Radiocarbon observations in atmospheric CO_2: determining fossil fuel CO_2 over Europe using Jungfraujoch observations as background. Sci Total Environ 391:211–216.

Martínez-Vilalta J, Sala A, Asensio D, Galiano L, Hoch G, Palacio S, Piper FI, Lloret F (2016) Dynamics of non-structural carbohydrates in terrestrial plants: a global synthesis. Ecol Monogr 86:495–516.

Michelot A, Simard S, Rathgeber C, Dufrêne E, Damesin C (2012) Comparing the intra-annual wood formation of three European species (*Fagus sylvatica*, *Quercus petraea* and *Pinus sylvestris*) as related to leaf phenology and non-structural carbohydrate dynamics. Tree Physiol 32:1033–1045.

Millard P, Sommerkorn M, Grelet GA (2007) Environmental change and carbon limitation in trees: a biochemical, ecophysiological and ecosystem appraisal. New Phytol 175:11–28.

Morris H, Plavcová L, Cvecko P et al. (2016) A global analysis of parenchyma tissue fractions in secondary xylem of seed plants. New Phytol 209:1553–1565.

Muhr J, Angert A, Negrón-Juárez RI, Muñoz WA, Kraemer G, Chambers JQ, Trumbore SE (2013) Carbon dioxide emitted from live stems of tropical trees is several years old. Tree Physiol 33:743–752.

Myers JA, Kitajima K (2007) Carbohydrate storage enhances seedling shade and stress tolerance in a neotropical forest. J Ecol 95: 383–395.

Nobuchi T, Sato T, Iwata R, Harada H (1984) Season of heartwood formation and the related cytological structure of ray parenchyma cells in *Robinia pseudoacacia* L. Mokuzai Gakkaishi 30:628–636.

Panchen ZA, Primack RB, Nordt B et al. (2014) Leaf out times of temperate woody plants are related to phylogeny, deciduousness, growth habit and wood anatomy. New Phytol 203: 1208–1219.

Plavcová L, Jansen S (2015) The role of xylem parenchyma in the storage and utilization of nonstructural carbohydrates. In: Hacke U (ed) Functional and ecological xylem anatomy. Springer International Publishing, Cham, Switzerland, pp 209–234.

Plavcová L, Hoch G, Morris H, Ghiasi S, Jansen S (2016) The amount of parenchyma and living fibers affects storage of nonstructural carbohydrates in young stems and roots of temperate trees. Am J Bot 103:603–612.

Richardson AD, Carbone MS, Keenan TF, Czimczik CI, Hollinger DY, Murakami P, Schaberg PG, Xu X (2013) Seasonal dynamics and age of stemwood nonstructural carbohydrates in temperate forest trees. New Phytol 197:850–861.

Richardson AD, Carbone MS, Huggett BA, Furze ME, Czimczik CI, Walker JC, Xu X, Schaberg PG, Murakami P (2015) Distribution and mixing of old and new nonstructural carbon in two temperate trees. New Phytol 206:590–597.

Sala A, Woodruff DR, Meinzer FC (2012) Carbon dynamics in trees: feast or famine? Tree Physiol 32:764–775.

Schädel C, Blöchl A, Richter A, Hoch G (2009) Short-term dynamics of nonstructural carbohydrates and hemicelluloses in young branches of temperate forest trees during bud break. Tree Physiol 29: 901–911.

Schuur EAG, Trumbore SE (2006) Partitioning sources of soil respiration in boreal black spruce forest using radiocarbon. Glob Chang Biol 12:165–176.

Smith MG, Miller RE, Arndt SK, Kasel S, Bennett LT (2017) Whole-tree distribution and temporal variation of non-structural carbohydrates in broadleaf evergreen trees. Tree Physiol 38:570–581.

Spicer R (2005) Senescence in secondary xylem: heartwood formation as an active developmental program. In: Holbrook NM, Zwieniecki MA (eds) Vascular transport in plants. Academic Press, Amsterdam, The Netherlands, pp 457–475.

Stewart CM (1966) Excretion and heartwood formation in living trees. Science 153:1068–1074.

Stokes A, Berthier S (2000) Irregular heartwood formation in *Pinus pinaster* Ait. is related to eccentric, radial, stem growth. For Ecol Manage 135:115–121.

Taneda H, Sperry JS (2008) A case-study of water transport in co-occurring ring- versus diffuse-porous trees: contrasts in water-status, conducting capacity, cavitation and vessel refilling. Tree Physiol 28:1641–1651.

R Development Core Team (2017) R: A language and environment for statistical computing. R Foundation for Statistical Computing, Vienna.

Terziev N, Boutelje J, Larsson K (1997) Seasonal fluctuations of low-molecular-weight sugars, starch, and nitrogen in sapwood of *Pinus sylvetris* L. Scand J For Res 12:216–224.

Trumbore S, Czimczik CI, Sierra CA, Muhr J, Xu X (2015) Nonstructural carbon dynamics and allocation relate to growth rate and leaf habit in California oaks. Tree Physiol 35:1206–1222.

Tulik M, Jura-Morawiec J, Bieniasz A, Marciszewska K (2019) How long do wood parenchyma cells live in the stem of a scots pine (*Pinus sylvestris* L.)? Studies on cell nuclei status along the radial and longitudinal stem axes. Forests 10:1–9.

Wason JW, Brodersen CR, Huggett BA (2019) The functional implications of tracheary connections across growth rings in four northern hardwood trees. Ann Bot 124:297–306.

Würth MKR, Peláez-Riedl S, Wright SJ, Körner C (2005) Non-structural carbohydrate pools in a tropical forest. Oecologia 143:11–24.

Xu X, Trumbore SE, Zheng S, Southon JR, McDuffee KE, Luttgen M, Liu JC (2007) Modifying a sealed tube zinc reduction method for preparation of AMS graphite targets: reducing background and attaining high precision. Nucl Instrum Methods Phys Res B 259:320–329.

Zhang H, Wang C, Wang X (2014) Spatial variations in non-structural carbohydrates in stems of twelve temperate tree species. Trees 28:77–89.

Ziegler H (1964) Storage, mobilization and distribution of reserve material in trees. In: Zimmermann M (ed) The formation of wood in forest trees. Academic Press, New York, NY, USA, pp 303–320.

Zimmermann MH (1983) Xylem structure and the ascent of sap. In: Timell T (ed) Springer series in wood science. Springer, Berlin, pp 4–149.